Nanoscale

Accepted Manuscript

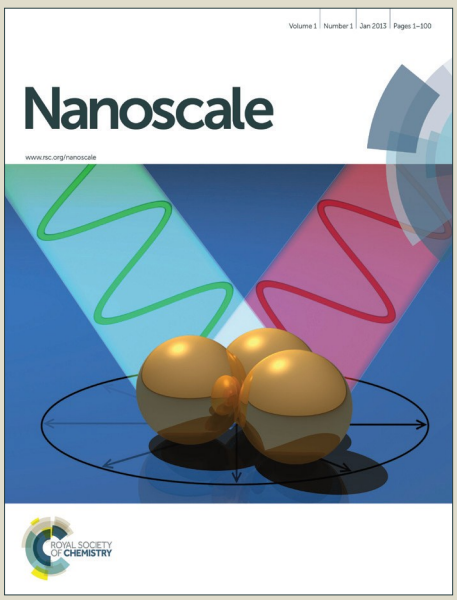

ROYAL SOCIETY OF CHEMISTRY

www.rsc.org/nanoscale

Journal Name

ARTICLE

Metal induced self-assembly of designed V-shape protein into 2D wavy supramolecular nanostructure

Received 00th January 20xx,
Accepted 00th January 20xx

DOI: 10.1039/x0xx00000x

www.rsc.org/

S. P. Qiao, C. Lang, R. D. Wang, X. M. Li, T. F. Yan, T. Z. Pan, L. L. Zhao, X. T. Fan, X. Zhang, C. X. Hou, Q. Luo, J. Y. Xu and J. Q. Liu*

In order to understand and imitate the more complex bio-process and fascinating functions in nature, protein self-assembly has been studied and attracts more and more interesting in recent years. The artificial protein self-assemblies have been constructed with many strategies. However, design of complicated protein self-assemblies utilizing the special profile of building blocks remains challenge. We herein report linear and 2D nanostructures constructed from V shape SMAC protein and induced by metal coordination. Zigzag nanowires and wavy 2D nanostructures have been demonstrated by AFM and TEM. The zigzag nanowires can translate to 2D nanostructure with excess metal ion, which reveals the step by step assembling process. Fluorescence and UV/Vis spectra have also been performed to further study the mechanism and process of self-assembling. Upon the protein nanostructure, fluorescence resonance energy transfer (FRET) could also be detected using fluorescein modified proteins as building blocks. This article provides an approach for designing and controlling self-assembled protein naostructures with distinctive topological mophology.

Introduction

In nature self-assembling proteins play key roles in biological functions. They control widely biological events from signal transduction, cell regulation to tissue formation. For example, endocytosis, the process used for packing and transporting external substances into cell, takes place with the help of clathrin coated vesicle which is assembled by clathrin protein.[1] As the cytoskeleton and muscle composition, microfilament and myofibrils are formed by self-assembling of actin protein.[2] The histone proteins help large amount of DNA co-assembling to form chromosome.[3] Therefore, for understanding the wisdom of nature, protein self-assembling and functionalization[4] have attracted lots of interests. As a more versertile and sophisticate building block, protein has been successfully arranged into 3D nanostructures by mediation of protein-protein interaction,[5] disulfide bridges,[6] covalent bond linker,[7] electrostatic interactions[8] and guest-host interaction.[9] By using the computational method and designing protein-protein interfaces, David Baker et al. described the design of cage-like protein assemblies.[10] Taking advantage of the guest-host interaction between heme and cytochrome b562, 1D and 2D self-assembled protein nanomaterials have been achieved by Takashi Hayashi and coworkers,[11] Induced by FGG tri-peptide tag and cucurbit[8]uril (CB[8]) guest-host interaction, our group also reported the successful construction of enzyme nanowires.[12]

Recent years, the metal-mediated interaction has received much attention for construction of defined protein self-assemblies. Taking advantages of convenient gene mutation, metal coordinate sites could be designed on specific location on the surface of protein building block, providing a strategy to control the orientation of interaction between proteins. F. Akif Tezcan and coworkers[13] first reported the successful use of metal coordination interaction[14] to direct protein assembly. 2D array of protein assembly were formed by designing the coordination motifs and interface of cytochrome b562, revealing a flexible method to control and modulate specific and complex protein assembly.[15] Up to now, metal coordination, as a stable, steerable and reversible interaction, has been proved to be a promising force to contribute to complex nanostructures.[16]

Although metal-mediated interaction have been reported to construct self-assembly, But utilizing the evolved V profile of protein in the nature and the stable interaction to construct more complicated 1D zigzag nanowires and corresponding 2D wavy nanostructures which are further self-assembled from 1D zigzag nanowires has been less reported. We know that the profile of building block has great influence on the morphology of protein assembly due to the “shape” could affect the growth orientation and local topology. Therefore, more complicated structure can be constructed with simpler computer simulation by making good use of the profile. We here select the SMAC protein, comes from mitochondrion of human beings and controls the cell apoptosis process[17] as building block. The complex zigzag, wavy structures can be constructed by arranging the V profile protein head-on and side by side simply, providing a way of constructing protein self-assembles with complex morphology. In addtion, compaired with other fluorescence resonance energy transfer (FRET) constructed

State Key Laboratory of Supramolecular Structure and Materials, College of Chemistry, Jilin University, Changchun 130012, China. E-mail: junqiuliu@jlu.edu.cn
† Electronic supplementary information (ESI) available: Experimental details, circular dichroism spectra, dynamic light scattering, additional AFM images and fluorescence spectra. See DOI: 10.1039/x0xx00000x

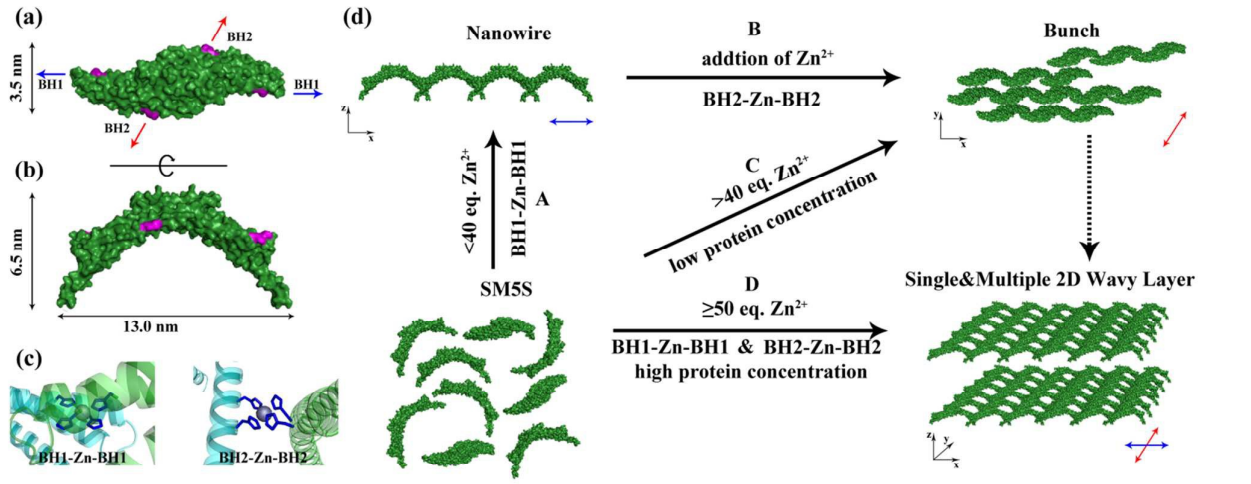

Fig. 1 top view (a) and side view (b) of SMAC-Mutation5Stop (SM5S) structure, four highlight histidines on each monomer form two bis-histidine motifs: BH1 (H75, H79) and BH2 (H137, H141). The direction of arrow shows the orientation of bis-histidine motifs bonding with Zn^{2+}. (c) shows the BH1-Zn-BH1 and BH2-Zn-BH2 centres when two SM5S equipped with Zn^{2+} at BH1 and BH2 site. (d) Different morphologies are obtained in different conditions. 1D nanowires were found when bis-histidine motifs are unsaturated with Zn^{2+}, blue arrow show the extending direction of nanowire benefiting from BH1-Zn-BH1 bond (process A); the bunch assemblies germinate due to the nanowire attaching with each other through BH2-Zn-BH2 interaction, the direction of growing is shown in red arrow (process B); when bis-histidine motifs are saturated with Zn^{2+}, assemblies extended in both blue and red arrows directions to form 2D nanostructures (process D).

on nature protein assemblys, the resulting stable nanostructures seem a novel artificial protein scaffold for building FRET system.

Herein we report a supramolecular system constructed by V profile protein as building block and induced by metal coordination interaction. The arch of SMAC protein is applied to construct zigzag and wavy protein assemblies, two bis-histidine motifs are accurately designed on each of SMAC monomer. Characterizied by AFM, TEM and spectrum measurements, the morphologies and forming process of the complex protein assemblies have been studied. Furthermore, we modified a pair of donor and acceptor chromophores onto distinguishing building blocks. The fluorescence resonance energy transfer (FRET) on the artificial protein assembly has been demonstrated successfully.

Results and discussion

Design, preparation and characterization of protein self-assembly

Following the approach that the profile of protein and well designed interaction will affect the morphology of protein self-assembly, we select SMAC, V shape protein, as our building block for construction of wavy nanostructure, and well design stable metal-mediated interaction to control the orientation and stabilize the nanostructures. The SMAC protein, consist of three α helix in each monomer, comes from mitochondrion of human beings and plays an important role in the apoptosis process[17], is C_2 symmetry homodimer protein with 115° angle. Therefore, the complicated zigag and wavy structures could been easily realized by arranging the V profile protein head-on and side by side, demonstrating the SMAC protein a suitable candidate for constructing wavy-like protein nanostructures. Previously study of Tezcan and coworkers has demonstrated a principle for designing coordination components on protein surface.[18] Taking advantage of computer simulation, we design two bis-histidine motifs: bis-histidine motif 1 (BH1) H75, H79 and bis-histidine motif 2 (BH2) H137, H141 on each monomer. The four bis-histidine motifs (in one dimer) are arranged in quadrilateral (Fig. 1a), this assures the protein assembly could extend in two directions to form 2D structure when coordinate with metal ions. Based on the arch profile of engineered SMAC protein and the stable metal-mediated interaction, the novel zigzag and 2D wavy-like nanostructure could be formed.

The protein with two bis-histidine motifs (SMAC-Mutation5-Stop) is engineered via site-mutation. The preparation, purification and characterization of SMAC-Mutation5-Stop (SM5S) and another protein variation, SMAC-Mutation4-Stop (SM4S) protein are reported in SI (Fig. S1). The final engineer protein, SM5S was characterized by Matrix-Assisted Laser Desorption Ionization Time of Flight Mass Spectrometry (MALDI-TOF-MS, Fig. S2): 20689.938 Da compared with the wild type SMAC: 20429Da, confirming the successful preparation of two variations. The circular dichroism spectrum is carried on to detect CD signals at neutral pH (Fig. S3). Data show no difference between three proteins, revealing that SM5S and SM4S maintain the same structure. The morphology of SMAC: V shape, with 13 nm in width, 6.5 nm in height and 3.5 nm in thickness from the crystal structure of wild type SMAC, which is shown in Fig. 1ab.[17]

To prove the formation of protein self-assembly and understand the significant role of Zn^{2+}, we use dynamic light scattering (DLS) to analyze the size distribution of protein assemblies. After incubation overnight at neutral pH with different concentrations of Zn^{2+}, the size-intensity curve of SM5S sample without Zn^{2+} show only one peak at about 10 nm, corresponding to hydration radius of dissociative dimer. In contrast, the distribution of sample with 20 equivalent Zn^{2+} obviously move toward larger size, and larger protein aggregates (above 1000nm) are found with 50, 100 equivalent Zn^{2+} (Fig. S4b). the DLS results demonstrate that the metal/protein ratio plays a vital role in the assembly. Future study is performed to understand the effects of reaction time on the size of assemblies. At the beginning, protein disperse in solution as

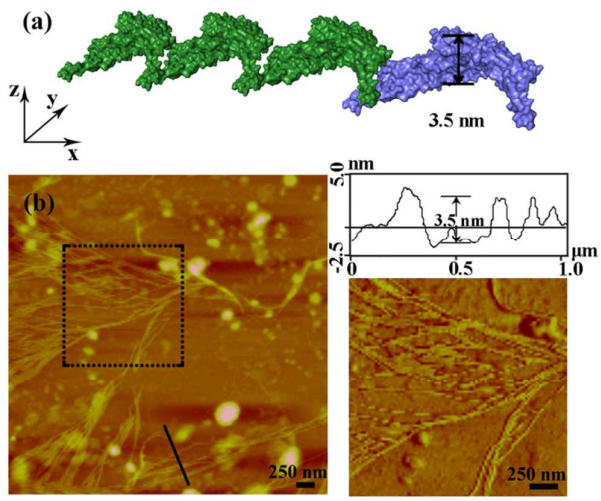

Fig. 2 Zn^{2+} induced self-assembly of SM5S detected by AFM with low metal/protein ratio. (a) The height of simulative assembly in PyMOL software is corresponding to the width of SM5S, 3.5nm. (b) AFM result when 20 equivalent Zn^{2+} was added into SM5S and dissociated nanowires were observed.

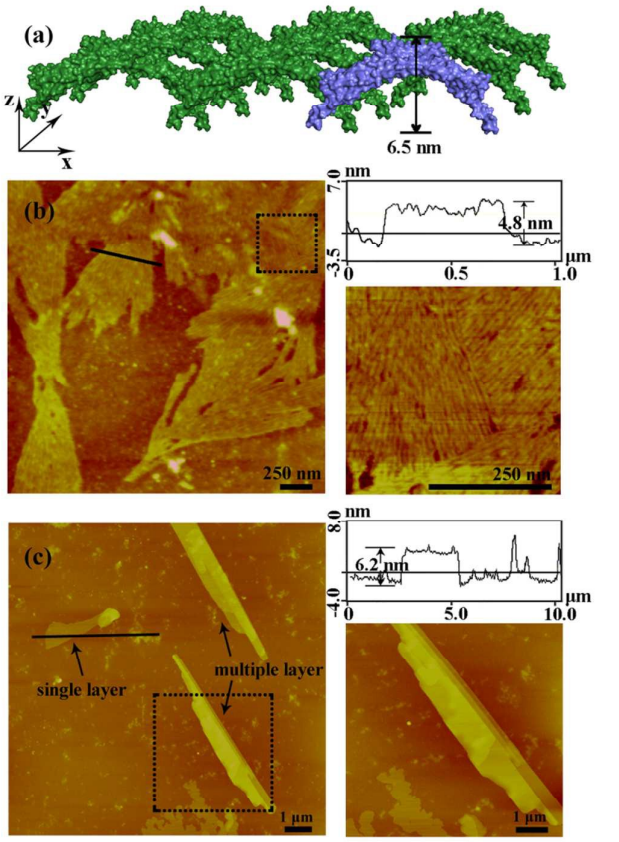

Fig. 3 AFM images of Zn^{2+} induced 2D protein nanostructures with high metal/protein ratio. (a) The height of simulative assembly in PyMOL software is corresponding to the height of SM5S, 6.5nm. (b) Increasing the metal/protein ratio to 40:1, linear zigzag assemblies further aggregate into 2D bundle nanowires. (c) With excess Zn^{2+} (50 eq.), large 2D-wavy single and multiple layers protein assemblies were found. Concentration of SM5S in (b) is 1μM while concentration in (c) is 10μM.

dissociative dimmer, after 1h, peak in intensity curve move toward 24nm, and the size of protein aggregation is enhanced inconspicuously in future time (Fig. S4c). Therefore, the size of protein self-assembly mainly depends on metal/protein ratio. Interestingly, the large aggregate disappear after adding chelator EDTA into the solution, revealing that the protein aggregates can self-assemble and disassemble reversibly through metal coordination (Fig. S4a).

After characterization of size distribution by DLS measurements, the morphology of metal induced protein assemblies have been studied by atomic force microscopy (AFM). The dissociative (Fig. 2), bundled zigzag nanowires, and 2D nanostructures with single, multiple layers (Fig. 3) are shown in AFM images. Notably, the height of dissociative zigzag nanowire in AFM images is 3.1 nm which is same as the thickness of single protein SM5S (3.5 nm), while the height of bundled zigzag nanowires and 2D wavy structure is about 4.3-6.6 nm, corresponding to the height of protein 6.5 nm. We assume that the SM5S building blocks in the dissociative nanowires may flat on the silicon wafer (Fig. 2a), while the protein in bundled zigzag nanowires and 2D wavy nanostructures stand on the silicon wafer (Fig. 3a). In addition, these nanowires prefer to attach with each other on identical plane rather than aggregate stochastically indicating there is special interaction in the perpendicular orientation. At high metal/protein ratio (metal:protein is 50), protein self-assemblies are observed by high resolution transmission electron microscope (TEM). Zoomed TEM images show the structural details and the "monomer" SM5S can also be found clearly in both 2D nanostructures. When protein concentration is low (1μM), bundle of nanowires are close-packed in the same plane (Fig. 4a, b). The width of each nanowire is about 3.1nm, which corresponding to the thickness of SM5S (3.5 nm). While the concentration of protein is 10μM, 2D wavy array is formed through two directions-extending of SM5S building blocks induced by coordination interaction (Fig. 4c). Therefore, depending on AFM and TEM results, we suppose that 2D nanostructures / array are formed by close-packing of dissociative nanowires and protein building blocks self-assemble in two directions respectively.

Understanding the process of self-assembling

To understand processes of protein assembly, we first focus on the two bis-histidine motifs engineered protein. With the help of two Zn^{2+} coordination sites, it should be possible to form protein assemblies in proper orientation. There are mainly three modalities to form Zn^{2+}-bonding-histidine4 centre between different proteins based on the spatial resistance: 1) BH2 from one and BH2 from another; 2) BH1 from one protein and BH1 from another; 3) BH1 from one and BH2 from another. Considering that protein would form a huge helix self-assemble in the third way, the CD measurement is performed (Fig. S3b). But the signal which could prove the existence of helix structure is not found, revealing that it is difficult to form BH1-Zn-BH2. Thus, the protein assembly is possibly induced by BH1-Zn-BH1 and BH2-Zn-BH2 bond.

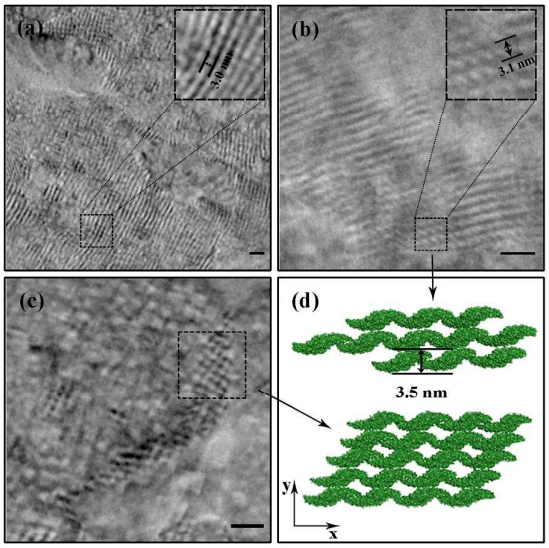

Fig. 4 TEM images of protein assemblies when Zn^{2+}/protein ratio is 50. Structures shown in (a) and (b) are consist of several strands of nanowires. The width of each strand is about 3.0 nm. (b) Monomer (SM5S) of nanowire was observed clearly in (b), indicating that SM5S may first form linear assemblies through BH1-Zn-BH1 centre and aggregate through BH2-Zn-BH2. Figure (c) demonstrates the detail of 2D arrays, protein could extend in two directions and wavy structure is clearly observed. Figure (d) shows the cartoon image illustrating two formation modes of 2D nanostructures. Each of scale bars is 10nm.

Then, the protein assembly system is analyzed by fluorescence and UV/Vis titration to further study the assembling process. We note that SM5S has the intrinsic fluorescence due to the existence of Trp residues. Taking advantage of Trp 78 residue next to the BH1, Fluorescence titration of SM5S can be employed to discuss the coordination and self-assembling mechanism.[19] Excited at 278nm, fluorescence signal is recorded from 300nm to 400nm at neutral pH. Fig. 5 shows that adding Zn^{2+} quenches the fluorescence intensity of SM5S (mutation site: D75H, Q79H, L137H, E141H), while another SMAC variant SM4S (mutation site: E76H, Q79H, L137H, E141H) quenches less (Fig. 5c, d). This indicates that quenching of fluorescence only depends on the interaction between Zn^{2+} and BH1 motif. We assume that interaction between Zn^{2+} and bis-histidine motifs may induce the combination of SM5S protein at BH1, forming a pair of Trp 78 residues with 1.3 nm distance (Fig. 5a, b). The Zn^{2+} between the Trp pair changes the microenvironment of Trp residue, resulting in quenching of fluorescent signal. In contract, fluorescence titration of SM4S quenches slightly, possibly due to longer distance between Trp residue pair and Zn^{2+} or the different binding modality. Thus, all fluorescence measurements reveal that SM5S prefers to connect with each other through BH1-Zn-BH1 centre.

UV/Vis titration results (Fig. 6) show an increasing UV absorbance of SM5S with higher Zn^{2+} concentration. We found that the increased rate of absorbance at 275nm changes obviously when metal/protein ratio is about 40 (Fig. 6b), this finding indicates that there are two stages of aggregation when Zn^{2+} induces the protein to form assemblies. Zn^{2+} tends to bond BH1 motifs of two SM5S first to form BH1-Zn-BH1 centre and then to form BH2-Zn-BH2 centre.

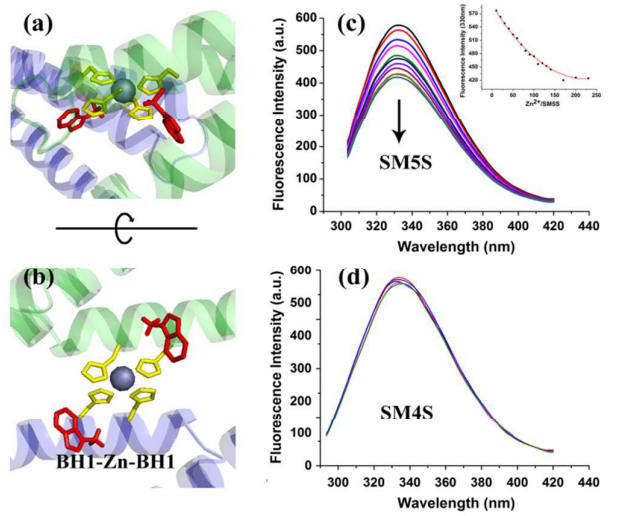

Fig. 5 (a-b) views of BH1-Zn-BH1 centre, highlight residues are two BH1 sites (yellow). The distance between two Trp residues (red) is about 1.3 nm. Zn^{2+} in the centre which changes the microenvironment of Trp residues results in fluorescence quenching of Trp. Fluorescence titration of SM5S (c) and SM4S (d) are performed by adding Zn^{2+}, fluorescence intensity of SM5S drops obviously with increasing Zn^{2+}, while the signal of SM4S hardly drops.

Based on all the results, we suppose there are two assembling pathway emerging in our protein assembly system and depended by the saturation of bis-histidine motifs, when bis-histidine motifs are unsaturated, Zn^{2+} prefer to binds BH1 motif, proteins first assemble into linear zigzag nanowires through BH1-Zn-BH1. With excess Zn^{2+}, the nanowires then attach each other through BH2-Zn-BH2 to form bundling nanowires. This step by step process is also proved by AFM and TEM; While bis-histidine motifs are saturated and protein concentration is high, protein can extend in two directions (along to BH1 and BH2 motifs) to form 2D nanostructures, which is also observed by AFM. Due to the V profile of building blocks, the 2D structures prefer a wavy rather than plane morphology. The complicated protein assemblies have also been verified by TEM. (Fig. 4)

Stability of protein assembly

Because the protein assembly is induced by metal coordination

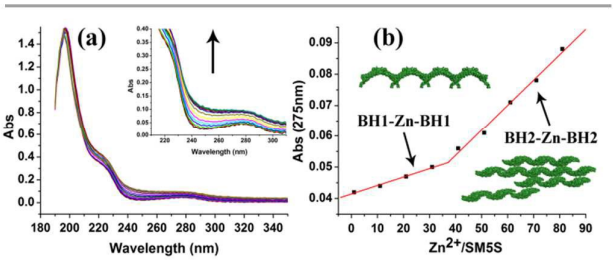

Fig. 6 (a) UV/Vis titration spectra of SM5S employed with increasing Zn^{2+}. The UV absorbance rises with adding more Zn^{2+}. (b) The curve which UV absorbance intensity at 275nm to different Zn^{2+}/protein ratio, shows a clear turn when Zn^{2+}/protein is above 40. The different slop reveals different bonding and aggregation modes[20].

interaction at multiple sites, the final compact 2D nanostructures may stabilize protein monomers. We expected that the protein assembly would be more tolerant of high temperature and denaturing agent. Thus, the CD measurements with increasing concentrations of denaturing agent (guanidine hydrochloride) are employed with both SM5S protein and the protein assembly induced by metal coordination to investigate the stability of supramolecular assemblies. Incubating in guanidine hydrochloride at objective concentration for 10 min, CD of SM5S protein (5μM) is recorded. Fig. S12 shows that the ratio of CD signal in 208nm and 222nm begins to raise fast, which demonstrates that α helix of SM5S protein starts to unfold. While 222nm/208nm raises slowly when adding denaturing agent into the metal induced protein assembly system, revealing that the protein in self-assembling system could be harder to unfold compared with monomer protein in the same concentration of denaturing agent. The metal induced assemblies are more stable than protein monomer until the concentration of guanidine hydrochloride reaches to 2M. Meanwhile, the thermal stability of protein nanostructure is also analysed by circular dichroism tests. CD spectra of SM5S and protein assembly are recorded each 5 degree from 30 to 95 degree. The folded-denature curves show that Tm has raised from 65 to 85 degree, revealing improvement of thermal stability (Fig. S13). These results demonstrate that assembling through metal coordination increase the stability of the system, also makes this system a potential candidate for biomaterial. The stability may benefit from limition of protein unfolding which result from metal tidily combining between protein monomers. Notably, this phenomenon provides an approach of further applications on biomaterial without the limitation of unstability.

FRET of protein assembly

Light harvesting system plays a vital role in nature due to the ability of conversion from light to chemical substance.[21] Energy transfer, which is one important process in light harvesting system, is realized through Fluorescence resonance energy transfer (FRET) event between chromophores with fine arrangement. To imitate the arrays of regularly chromophores, Matthew B. Francis and coworkers first successfully construct a series of outstanding light harvesting using modified nature protein assembly as scaffold.[22] The highly ordered protein self-assembly could hang chromophores for optimal energy transfer and prevent contact quenching in the meantime. Therefore, protein assembly would be an appropriate scaffold for construction of FRET system.

The highly ordered arrangement and stability makes our artificial protein self-assembly an ideal scaffold for construction of light harvesting system. Thus, we construct two kinds of protein building blocks by connecting amino-reactive chromophore-isothiocyanate (donor and acceptor) to SM5S protein. After Induced by metal-mediated interaction, chromophore-modified protein self-assembly could be formed, on account of the close space between chromophore-modified proteins, fluorescence resonance energy transfer (FRET) could be realized. It is worth noting that we use “modified then assembling” rather than “assembling then modified” schema on the artificial assembly because we could accurately control the chromophore ratio for characterization of our FRET system, even though this schema would affect the assembly efficiency of building block and the final energy transfer efficiency between donor and acceptor.

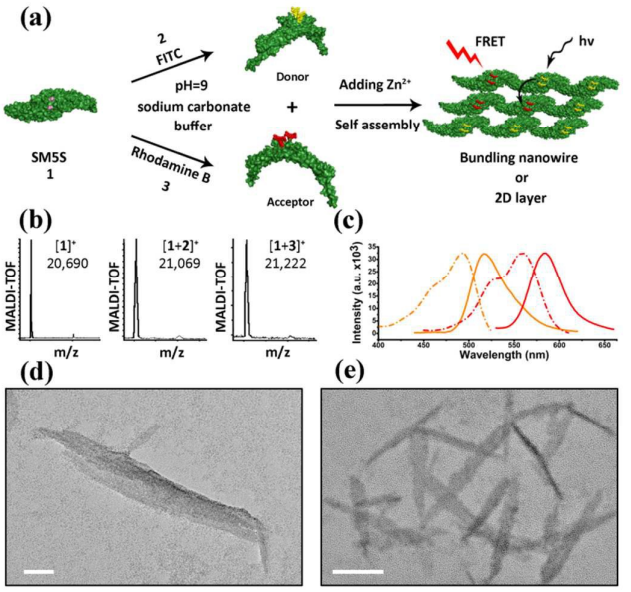

Fig. 7 (a) Schema of constructing FRET system: donor (FITC) and acceptor (rhodamine B) are first linked to SM5S, and protein self-assemblies are then induced by metal coordination. (b) MALDI-TOF results of SM5S, SM5S-FITC (SF) and SM5S-rhodamine B (SRB) reveal that two chromophores have been modified onto proteins. (c) Emission (solid line) and excitation (dash line) spectra of SF protein (orange) and SRB protein (red). Obvious overlap between the excitation of SRB and emission of SF could be observed. (d) TEM images of the SM5S-Zn^{2+} protein assembly and (e) Modified-SM5S-Zn^{2+} assembly in FRET system. The morphologies of both assemblies are similar. The scale bars are 50 nm.

We herein select FITC as the donor and rhodamine B as the acceptor since the appropriate degree of the overlap between emission of FITC (maximum absorption at 497nm, maximum emission at 510 nm) and absorption of rhodamine B (maximum absorption at 554nm and emission at 584 nm), which allow FRET easier to occur from donor to acceptor, (shown in Fig. S7). FITC and rhodamine B are modified to proteins at pH=9.0 for 8h by mild reactions.[23] The modified two proteins SF (SM5S-FITC), SRB (SM5S-rhodamine B) were confirmed by Matrix-Assisted Laser Desorption Ionization Time of Flight Mass Spectrometry (Fig. S8, S9), revealing that we have obtained the two kinds of chromophore-modified proteins. Mixing SF with SRB protein at different ratios and ascertained by the excitation spectra (Fig. S10), chromophore-modified protein self-assemblies are prepared by metal-mediated interaction. Characterizied by TEM, the resulting protein assemblies are shown that they have the similar morphology (Fig. 7e) as the 2D nanostructure we have obtained before (Fig. 7d).

To estimate the Förster radius of two chromophores in the FRET system we constructed, the fluorescence quantum yield of chromophore modified protein (SF and SRB) was determined by the method reported by Williams et al. [24] (Fig. S10). The spectral overlap integral was first calculated using the following equation:[25]

$$J(\lambda) = \int_0^\infty F_D(\lambda)\varepsilon_A(\lambda)\lambda^4 d\lambda$$

TABLE 1. Donor-Donor and Donor-Acceptor Pair Results

Donor-donor/ acceptor pair	Φ_D (donor)	J (10^{15} $M^{-1}cm^{-1}nm^4$)	R_0 (nm)	r (nm)	E (%)
SF-SF	0.256	1.90	4.35.	7.93	2.7
SRB-SRB	0.185	4.04	5.19	3.28	94
SF-SRB	0.256	4.70	5.32	4.53	72

where λ is the wavelength (nm), εA is the unity absorptivity of the acceptor at that wavelength (M-1 cm-1) and FD is the emission spectrum of donor normalized on the wavelength scale as followed

$$1 = \int_0^\infty F_D(\lambda)d\lambda$$

The overlap integral for transfer between FITC and rhodamine B, two FITC molecules and two rhodamine B molecules were calculated to be $4.70x10^{15}$, $1.92x10^{15}$ and $4.04x10^{15}$ $M^{-1}cm^{-1}nm^4$ respectively (Table 1).

Assuming a value of 2/3 for the orientation value κ^2, an aqueous refractive index of η = 1.33, and considering the unit overlap integral J described above, the Förster radius (R_0), the theoretical donor-acceptor distance at 50% energy transfer efficiency, was calculated using the following equation:[26]

$$R_0 = 0.211(\kappa^2 n^{-4} Q_D J(\lambda))^{1/6} (\text{in Å})$$

where Q_D is the quantum yield of the donor. Therefore, the Förster radius was found to be 5.3 nm for transfer between the FITC and rhodamine B molecules.

The donor-acceptor distance (r) was thus estimated to be 4.5 nm by structural model in software Pymol. We finally get the efficiency of energy transfer (E) using the following equation:[26]

$$E = \frac{R_0^6}{R_0^6 + r^6}$$

The high efficiency of energy transfer between the FITC and rhodamine B chromophores is 72%

For detecting the FRET event from FITC to rhodamine B, the emission spectra of SF-SRB system are detected[27] before (Fig. S11) and after self-assembling induced by metal-mediated interaction (Fig. 8). In order to affirm the quenching of FITC caused by rhodamine B, increasing SRB protein and invariant SF protein are mixed and self-assembled through metal coordination, the emission of donor FITC conspicuously decrease and the emission of acceptor increase. Meanwhile, the emission of acceptor also could enhance when adding donor in system and assembling. All results reveal that FRET do occur in this system: the energy transform from donor to acceptor resulting in the quenching of donor emission and enhancing of acceptor emission. It also demonstrates that the novel protein nanostructure we designed is a promising artificial scaffold for construction of FRET system.

Conclusion

We herein report the successful construction of complicated zigzag and 2D-wavy protein self-assembling system utlizing V profile of protein building block and coordination interaction. Zigzag nanowires, 2D wavy nanostructures are obtained at different metal/protein ratio. The protein self-assemblies have been studied by DLS, AFM, TEM, fluorescent and UV/Vis spectra in order to understand the process of self-assembling and morphology of protein self-assemblies. The complex 2D wavy nanostructures benefit from V profile of building block and designed metal coordination interaction, demonstrating an approach on construction of complicated protein nanostructure. Upon the stability of protein assembly compared with dissociative protein monomer, the FRET system has been successfully realized using the artificial protein self-assembly as scaffold, This shows the novel designed protein assembly a promising frame for light harvesting system, we anticipate its further applications in biomaterials.

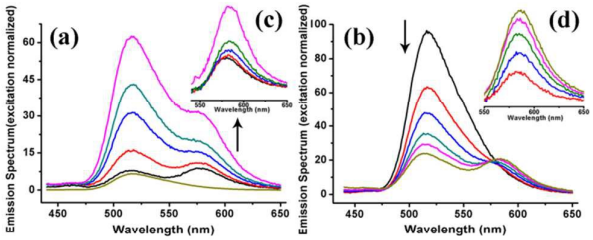

Fig. 8 Normalized Emission spectra of FRET system constructed by using SF and SRB proteins as building blocks. (a) Emission of SRB raise with addition SF into system (normalized at 570nm of acceptor excitation), confirming that FRET event take place. (b) Increasing amounts of the acceptor results in an obvious quenching of donor and increasing of acceptor emission duo to the FRET event. (c, d) the resulting acceptor emission spectra obtained by removing the FITC emission peak from (a) and (b), showing a raising emission of acceptor.

Experimental procedures

Construction and expression of SMAC variants SMAC-Mutation4-stop & SMAC-Mutation5-stop

Depending on the computer simulation, the bis-histidine motifs are designed on the surface of protein, the protein crystal structure was viewed in property distance and orientation in software PyMol. Two variants are obtained through four point mutations, primers used for point mutation is shown in tableS1. The final DNA sequence is confirmed by genetic sequencing before expression. Three kinds of protein are expressed in Escherichia Coli strain BL21(ED3), incubating in 5ml LB liquid medium including Kanamycin (100 μg/mL) overnight, cells are inoculated into 500ml LB liquid medium containing kanamycin (100μg/mL) until OD600 is about 0.1 and incubated till OD600 is about 0.6-0.8. Then IPTG was added to the final concentration of 1mM and the cells were incubated for 4 hours. Collected by centrifugation, cells were ultrasonicated and remove sediment by centrifugation, the soluble fraction is purified over anion-exchange chromatography (DEAE) and further purification was performed on G75 and G25 to remove nucleinic acid and salt.

DLS measurement

DLS was performed to study protein self-assembly process. SM5S was dissolved in TBS buffer (10mM Tris, pH8.5), the final concentration is about 1μM, samples were made with addition of different Zn^{2+} concentration (0μM, 20μM, 40μM, 50μM, 100μM) and incubated overnight prior to DLS measurement (Fig. S4a). The influence of assembling time on the size of protein self-assemblies was also studied by DLS. Dissolved in TBS and adding 20eq. Zn^{2+}, the DLS signal of sample was recorded during 4 hours.

AFM imaging

Protein assemblies were made by dissolving SM5S in Tris-HCl buffer pH=8.5 15mM (TBS) followed by adding Zn^{2+} and incubating overnight. All the sample were prepared by dropping 10μl solution on silicon slice which have been hydroxylated and adsorb for 10 min, then wash the silicon slice three times using water, air dried before employing on AFM. During the AFM imaging, taping mode is used with 0.8Hz scan speed.

TEM characterization

TEM imaging was used to study morphology of protein self-assemblies. The sample was prepared by placing a drop of the samples on a 300-mesh, carbon-coated copper grid for 10 min, after negative stained by 4% Sodium phosphotungstate for 40s, samples were dried in air before measurement. The observation was performed with a JEOL1011 transmission electron microscope operating with an acceleration voltage of 200 kV.

Spectroscopy measurements

Fluorescence and UV/Vis titrations were performed as follows. SM5S and SM4S were dissolved in TBS with final concentration of 1μm, 1μl of 10mM Zn^{2+} was added in 1ml sample each time. Then the system was incubated for 2 min before recording fluorescence signal. Excited is at 278nm, both slit widths are 10nm, and fluorescence signal is recorded from 300nm to 400nm at pH8.5 (10mM Tris-HCl buffer). Similarly, UV/Vis spectrum was also performed under the same conditions and UV results were recorded from 190nm to 350nm. To detect the changes on second structure and stability in high temperature or organic solvent, CD measurements were employed. All the samples contain 20mM TBS, 200mM NaCl and protein with different concentrations. For studying the thermostability, CD signal were recorded from 190nm to 260nm where contain the information of second structure. Large range CD was also performed to detect the CD signal of protein assemblies.

Acknowledgements

This work was supported by the Natural Science Foundation of China (No: 21234004, 21420102007, 21574056, 21221063), 111 project (B06009), the Chang Jiang Scholars Program of China.

Notes and references

1 M. K. Higgins and H. T. McMahon, *Trends in Biochemical Sciences*, 2002, **27**, 257–63.

2 G. J. Doherty and H. T. McMahon, *Annu. Rev. Biophys.*, 2008, **37**, 65–95.

3 B. Guillemette, A. R. Bataille, N. Gévry, M. Adam, M. Blanchette, F. Robert and L. Gaudreau, *PLoS Biol.*, 2005, **3**, 2100-2110.

4 (a) N. J. M. Sanghamitra and T. Ueno, *Chem. Commun.*, 2013, **49**, 4114-4126; (b) B. Maity, K. Fujita and T. Ueno, *Curr. Opin. Chem. Biol.*, 2015, **25**, 88-97; (c) T. Ueno, *J. Mater. Chem.*, 2008, **18**, 3741–3745.

5 (a) J. C. Sinclair, K. M. Davies, C. Ve´nien-Bryan and M. E. M. Noble, *Nat. Nanotechnol.*, 2011, **6**, 558-562; (b) J. F. Graveland-Bikker, R. I. Koning, H. K. Koerten, R. B. J. Geels, R. M. A. Heerenc and C. G. de Kruif, *Soft Matter*, 2009, **5**, 2020-2026; (c) C. R. Bourne, S. P. Katen, M. R. Fulz, C. Packianathan and A. Zlotnick, *Biochemistry*, 2009, **48**, 1736-1742; (d) Y. I Maeda and H. Matsui, *Soft Matter*, 2012, **8**, 7533-7544; (e) M. Dalmau, S. Lim and S. Wang, Nano Lett., 2009,**9**, 160-166; (f) Z. Liu, J. Qiao, Z. W. Niu and Q. Wang, *Chem. Soc. Rev.*, 2012, **41**, 6178-6194.

6 (a) K. Oohora, S. Burazerovic, A. Onoda, Y. M. Wilson, T. R. Ward and T. Hayashi, *Angew. Chem., Int. Ed.*, 2012, **51**, 3818-3821; (b) W. A. Petka, J. L. Harden, K. P. McGrath, D. Wirtz and D. A. Tirrell, *science*, 1998, **281**, 389-392; (c) T. T. H. Pham, P. J. Skrzeszewska, M. W. T. Werten, W. H. Rombouts, M. A. C.S tuart, F. A. deWolfb and J. vander Gucht, *Soft Matter*, 2013, **9**, 6391-6397.

7 (a) M. M. Ma and D. Bong, *Org. Biomol. Chem.*, 2011, **9**, 7296-7299; (b) K. Oohora, A. Onoda and T. Hayashi, *Chem. Commun.*, 2012, **48**, 11714-11726; (c) L. Arce, M. Zosugagh, C. Arce, A. Moreno, A. Ros and M. Valca´rcel, *Biosens. Bioelectron.*, 2007, **22**, 3217-3223; (d) Z. Matharu, A. J. Bandodkar, G. Sumana, P. R. Solanki, E. M. I. MalaEkanayake, K. Kaneto, V. Gupta and B. D. Malhotra, *J. Phys. Chem. B*, 2009, **113**, 14405-14412; (e) A. G. Mantzila, V. M. and M. I. Prodromidis, *Anal. Chem.*, 2008, **80**, 1169-1175; (f) A. Herrmann, *Chem. Soc. Rev.*, 2014, **43**, 1899-1933.

8 (a) L. Miao, J. S. Han, H. Zhang, L. L. Zhao, C. Y. Si, X. Y. Zhang, C. X. Hou, Q. Luo, J. Y. Xu, and J. Q. Liu, *ACS Nano*, 2014, **4**, 3743-3751; (b) C. Chen, K. M. Bromley, J. Moradian-Oldak and J. J. DeYoreo, *J. Am. Chem. Soc.*, 2011, **133**, 17406-17413; (c) M. A. Kostiainen, P. Hiekkataipale, A. Laiho, V. Lemieux, J. Seitsonen, J. Ruokolainen and P. Ceci, *Nat. Nanotechnol.*, 2013, **8**, 52-56.

9 (a) M. Ramaekers, S. P. W. Wijnands, J. L. J. van Dongen, L. Brunsveld and P. Y. W. Dankers, *Chem. Commun.*, 2015, **51**, 3147-3150; (b) J. C. T. Carlson, S. S. Jena, M. Flenniken, T. Chou, R. A. Siegel and C. R. Wagner, *J. Am. Chem. Soc.*, 2006, **128**, 7630-7638; (c) H. Kitagishi, K. Oohora and T. Hayashi, *Biopolymers*, 2009, **91**, 194–200; (d) H. Kitagishi, Y. Kakikura, H. Yamaguchi, K. Oohora, A. Harada and T. Hayashi, *Angew. Chem., Int. Ed.*, 2009, **48**, 1271–1274; (e) K. Oohora, A. Onoda, H. Kitagishi, H. Yamaguchi, A. Haradacand T. Hayashi, *Chem. Sci.*, 2011, **2**, 1033–1038.

10 N. P. King, W. Sheffler, M. R. Sawaya, B. S. Vollmar, J. P. Sumida, I. André, T. Gonen, T. O. Yeates and D. Baker, *science*, **336**, 1171-1174.

11 H. Kitagishi, K. Oohora, H. Yamaguchi, H. Sato, T. Matsuo, A. Harada and T. Hayashi, *J. Am. Chem. Soc.*, 2007, **129**, 10326–10327.

12 C. X. Hou, J. X. Li, L. L. Zhao, W. Zhang, Q. Luo, Z. Y. Dong, J. Y. Xu and J. Q. Liu, *Angew. Chem., Int. Ed.*, 2013, **52**, 5590-5593.

13 (a) R. J. Radford, M. Lawrenz, P. C. Nguyen, J. A. McCammon and F. A. Tezcan, *Chem. Commun.*, 2011, **47**, 313-315; (b) R. J. Radford and F. A. Tezcan, *J. Am. Chem. Soc.*, 2009, **131**, 9136–9137; (c) D. N. Woolfson and Z. N. Mahmoud, *Chem. Soc. Rev.*, 2010, **39**, 3464–3479.(d) A. L. Boyle and D. N. Woolfson, *Chem. Soc. Rev.*, 2011,**40**, 4295-4306.

14 (a) D. J. E. Huard, K. M. Kane and F. A. Tezcan, *Nat. Chem. Biol.*, 2013, **9**, 169-176; (b) Y. S. Bai, Q. Luo, W. Zhang, L. Miao, J. Y. Xu, H. B. Li and J. Q. Liu, *J. Am. Chem. Soc.*, 2013, **135**, 10966–10969.

15 J. D. Brodin, J. R. Carr, P. A. Sontz, and F. A. Tezcan, *PNAS*, 2014, **111**, 2897-2902.

16 J. D. Brodin, X. I. Ambroggio, C. Tang, K. N. Parent1, T. S. Baker and F. A. Tezcan, *Nat. Chem.*, 2012, **4**, 375-382.
17 (a) J. J. Chai, C. Y. Du, J. W. Wu, S. Kyin, X. D. Wang and Y. G. Shi, *Nature*, 2000, **406**, 855-862; (b) H. Y. Sun, Z. Nikolovska-Coleska, J. F. Lu, J. L. Meagher, C. Y. Yang, S. Qiu, Y. Tomita, Y. Ueda, S. Jiang, K. Krajewski, P. P. Roller, J. A. Stuckey and S. M. Wang, *J. Am. Chem. Soc.*, 2007, **129**, 15279-15294; (c) D. R. Green, *Cell*, 2000, **102**, 1–4; (d) D. Potenza, L. Belvisi, F. Vasile, E. Moroni, F. Cossu and P. Seneci, *Org. Biomol. Chem.*, 2012, **10**, 3278–3287.
18 E. N. Salgado, R. J. Radford, and F. A. Tezcan, *Acc. Chem. Res.*, 2010, **43**, 661-672.
19 (a) R. Yang, L. Chen, T. Zhang, S. Yang, X. Leng and G. Zhao, *Chem. Commun.*, 2014, **50**, 481-483; (b) H. Shen, Z. Gu, K. Jian, J. Qi, *J. Pharmaceut. Biomed.*, 2013, **75**, 86–93; (c) F. Bou-Abdallah, G. H. Zhao, G. Biasiotto, M. Poli, P. Arosio and N. D. Chasteen, *J. Am. Chem. Soc.*, 2008, 130, 17801–17811; (d) R. Yang, L. Chen, S. Yang, C. Lv, X. Leng and G. Zhao, *Chem. Commun.*, 2014, **50**, 2879—2882.
20 (a) C. C. Decandio, E. R. Silva, I. W. Hamley, V. Castelletto, M. S. Liberato, V. X. Oliveira, Jr., C. L. P. Oliveira, and W. A. Alves, *Langmuir*, 2015, **31**, 4513-4523; (b) C. Yuan, J. Chen, S. Yu, Y. Chang, J. Mao, Y. Xu, W. Luo, B. Zeng and L. Dai, *Soft Matter*,2015, **11**, 2243–2250.
21 (a) X. D. Liu, Y. G. Shen, *FEBS Lett.*, 2004, **569**, 337–340; (b) B. Andersson, D. H. Yang and H. Paulsen, *FEBS Lett.*, 2000, **466**, 385–388.
22 (a) T. L. Schlick, Z. Ding, E. W. Kovacs and M. B. Francis, *J. Am. Chem. Soc.*, 2005, **127**, 3718-3723; (b) R. A. Miller, A. D. Presley and M. B. Francis, *J. Am. Chem. Soc.*, 2007, **129**, 3104-3109; (c) R. A. Miller, N. Stephanopoulos, J. M. McFarl and A. S. Rosko, P. L. Geissler and M. B. Francis, *J. Am. Chem. Soc.*, 2010, **132**, 6068-6074; (d) M. T. Dedeo, K. E. Duderstadt, J. M. Berger and M. B. Francis, *Nano Lett.*,2010, **10**, 181-186; (e) A. C. Obermeyer, S. L. Capehart, J. B. Jarman and M. B. Francis, *PLoS ONE*, 2014, **9**, e100678.
23 V. Levi, F. L. Gonzalez Flecha, *BBA.*, 2002, **1599**, 141–148
24 L. Mottram, S. Boonyarattanakalin, R. E. Kovel and B. R. Peterson, *Org. Lett.*, 2006, **8**, 581–584.
25 A. Montali, G. S. Harms, A. Renn, C. Weder, P. Smith, and U. P. Wild, *Phys. Chem. Chem. Phys.*, 1999, **1**, 5697–5702.
26 J. R. Lakowicz, *Principles of Fluorescence Spectroscopy*, Plenum Press: New York, 1983; pp 446-447.
27 (a)N. Stephanopoulos, Z. M. Carrico and M. B. Francis, *Angew. Chem. Int. Ed.*, 2009, **48**, 9498 –9502; (b) Y. S. Nam, T. Shin, H. Park, A. P. Magyar, K. Choi, G. Fantner, K. A. Nelsonand A. M. Belcher, *J. Am. Chem. Soc.*, 2010, **132**, 1462–1463; (c) F. Pu, L. Wu, E. G. Ju, X. Ran, J. S. Ren and X. G. Qu, *Adv. Funct. Mater.*, 2014, **24**, 4549–4555; (d) Y. Zhang, H. Y. Zhang, J. Hollins, M. E. Webb and D. J. Zhou, *Phys. Chem. Chem. Phys.*, 2011,**13**, 19427-19436.